

Environmental Control of Tropical Cyclone Intensity

KERRY EMANUEL, CHRISTOPHER DESAUTELS, CHRISTOPHER HOLLOWAY, AND ROBERT KORTY

Program in Atmospheres, Oceans, and Climate, Massachusetts Institute of Technology, Cambridge, Massachusetts

(Manuscript received 7 April 2003, in final form 5 November 2003)

ABSTRACT

The influence of various environmental factors on tropical cyclone intensity is explored using a simple coupled ocean–atmosphere model. It is first demonstrated that this model is capable of accurately replicating the intensity evolution of storms that move over oceans whose upper thermal structure is not far from monthly mean climatology and that are relatively unaffected by environmental wind shear. A parameterization of the effects of environmental wind shear is then developed and shown to work reasonably well in several cases for which the magnitude of the shear is relatively well known. When used for real-time forecasting guidance, the model is shown to perform better than other existing numerical models while being competitive with statistical methods. In the context of a limited number of case studies, the model is used to explore the sensitivity of storm intensity to its initialization and to a number of environmental factors, including potential intensity, storm track, wind shear, upper-ocean thermal structure, bathymetry, and land surface characteristics. All of these factors are shown to influence storm intensity, with their relative contributions varying greatly in space and time. It is argued that, in most cases, the greatest source of uncertainty in forecasts of storm intensity is uncertainty in forecast values of the environmental wind shear, the presence of which also reduces the inherent predictability of storm intensity.

1. Introduction

Forecasts of hurricane movement have improved steadily over the last three decades owing to a combination of better observations and much improved numerical models (DeMaria and Kaplan 1997). By contrast, there has been comparatively little advance in predictions of intensity (as measured, e.g., by maximum surface wind speed) in spite of the application of sophisticated numerical models (DeMaria and Kaplan 1997). The best intensity forecasts today are statistically based (DeMaria and Kaplan 1994). While there is much hope that three-dimensional coupled models will lead to better understanding of the factors that control hurricane intensity and to increased skill of hurricane intensity forecasts (Bender and Ginis 2000), at present models do not have enough horizontal resolution to capture the full magnitude of intense storms. Experiments with research-quality three-dimensional numerical models show nontrivial dependence of model storm intensity on horizontal resolution even at grid spacings as small as 1–2 km (Shuyi Chen 2002, personal communication). Fortunately, it is probably not necessary to capture full storm intensity in order to achieve good track forecasts.

Changes in tropical cyclone intensity may be loosely partitioned between changes arising from changing conditions of the storm's environment and internal fluctu-

ations that may reflect storm-scale instabilities or the stochastic effects of high-frequency transients such as moist convection. Concentric eyewall cycles are known to be associated with sometimes dramatic changes in storm intensity (Willoughby and Black 1996), although it is not yet clear whether these are manifestations of strictly internal instabilities or are triggered and/or controlled by the large-scale environment. Work by Molinari and Vollaro (1989, 1990) and Nong and Emanuel (2003) suggests that eyewall cycles may be triggered by environmental influences but, once initiated, develop autonomously. Owing to the relatively short time scales of phenomena like these, their dominance in tropical cyclone intensity change would compromise predictability on such time scales. We here take as our working premise that internal fluctuations are generally of secondary importance in tropical cyclone intensity change. We test this premise by attempting to predict intensity change using a model whose behavior is largely controlled by external environmental factors.

The majority of the research literature on hurricane intensity focuses on the prestorm thermodynamic environment (e.g., Emanuel 1986, 1988; Bister and Emanuel 1998), and certain properties of the atmospheric environment, such as the vertical shear of the horizontal wind (e.g., Jones 2000; Frank and Ritchie 2001), and dynamical features, such as disturbances in the upper troposphere (e.g., Molinari and Vollaro 1989, 1990, 1995). This remains so even though it is well known that hurricanes alter the surface temperature of the ocean

Corresponding author address: Kerry Emanuel, MIT, Room 54-1620, 77 Massachusetts Ave., Cambridge, MA 02139.
E-mail: emanuel@texmex.mit.edu

over which they pass (Price 1981) and that a mere 2.5-K decrease in ocean surface temperature near the core of the storm would suffice to shut down energy production entirely (Gallacher et al. 1989). Simulations with three-dimensional coupled atmosphere–ocean models (Gallacher et al. 1989; Khain and Ginis 1991; Schade and Emanuel 1999) confirm that interaction with the ocean is a strong negative feedback on storm intensity.

The weight given in the literature to strictly atmospheric environmental factors reflects a poor collective understanding of the relative importance of the various processes to which tropical cyclone intensity change has been ascribed. The best statistical prediction schemes account for prestorm sea surface temperature and vertical wind shear but do not account for feedback from ocean interaction.

In this paper, we employ a simple but skillful coupled atmosphere–ocean tropical cyclone model to explore the sensitivity of tropical cyclone intensity to various environmental factors. The atmospheric model is phrased in potential radius coordinates, permitting exceptionally high horizontal resolution in the eyewall, where it is needed, at low computational cost. This model is coupled to a simple one-dimensional ocean model, which has been shown to mimic almost perfectly the feedback effect of a fully three-dimensional ocean model. We first demonstrate that this coupled model is capable of accurately simulating the intensity evolution of storms that move over an ocean whose upper thermal structure is close to climatology and that are unmolested by vertical shear of the environmental wind. We then develop an empirical parameterization of the effects of wind shear, using data from a few storms for which the environmental shear is relatively well known, and show that this parameterization is effective in several cases for which shear was the dominant factor inhibiting storm intensity. Finally, the coupled model is used to explore the effects of various environmental factors in controlling the intensity evolution of a limited number of events selected to illustrate these factors.

2. Model design

a. Atmospheric model

The atmospheric model is described in detail by Emanuel (1995a). It is constructed on the assumption that the storm is axisymmetric, that the airflow is in hydrostatic and gradient wind balance, and that the vortex is always close to a state of neutral stability to slantwise convection in which the temperature lapse rate is everywhere and always assumed to be moist adiabatic along angular momentum surfaces. Thus, the saturated moist potential vorticity is zero everywhere, and the balance conditions allow this quantity to be inverted, subject to certain boundary conditions (Shutts 1981; Emanuel 1986). These constraints place strong restric-

tions on the structure of the vortex so that, with the exception of the water vapor distribution, the vertical structure is determined by the radial distribution of boundary layer moist entropy and by the vorticity at the tropopause. The water vapor distribution is characterized by the moist entropy of the boundary layer and of a single layer in the middle troposphere.

Moist convection is represented by one-dimensional updraft and downdraft plumes, whose mass flux is determined to insure approximate entropy equilibrium of the boundary layer (Raymond 1995) and for which the precipitation efficiency is taken to be a function of the environmental relative humidity in the middle troposphere. The saturation moist entropy above the boundary layer (and along angular momentum surfaces) closely follows the boundary layer moist entropy in regions of convection but is determined by large-scale subsidence and radiative cooling in regions, such as the eye, that are stable to moist convection.

The model variables are phrased in “potential radius” coordinates (Schubert and Hack 1983). Potential radius (R) is proportional to the square root of the absolute angular momentum per unit mass about the storm center and is defined by

$$fR^2 = 2rV + fr^2, \quad (1)$$

where r is the physical radius, V is the azimuthal velocity, and f is the Coriolis parameter. In the runs presented here, there are 50 nodes that span 1000 km, giving an average resolution of 20 km; however, the resolution is substantially finer than this in regions of high vorticity, such as the eyewall, and can be as fine as 1–2 km in the eyewalls of intense storms.

When run with a fixed sea surface temperature and a fixed atmospheric environment, the steady-state storm intensity is controlled strictly by the potential intensity, which is a function of sea surface temperature, storm-top environmental temperature, and air–sea thermodynamic disequilibrium alone. The potential intensity is the maximum steady intensity a storm can achieve based on its energy cycle, in which the heat input by evaporation from the ocean and from dissipative heating, multiplied by a thermodynamic efficiency, is balanced by mechanical dissipation in the storm’s atmospheric boundary layer (Bister and Emanuel 1998). We stress that the steady-state intensity behavior in this model is controlled only by the potential intensity; the particular combination of sea surface and outflow temperatures and air–sea disequilibrium is immaterial.

One potentially important source of uncertainty is the formulation of the surface fluxes of enthalpy and momentum to which the evolution of storm intensity is sensitive (Emanuel 1995b). The model uses classical bulk aerodynamic flux formulas based on the near-surface gradient wind speed. After some experimentation, we found that good simulations are obtained using enthalpy and momentum transfer coefficients that are equal to each other and increase linearly with gradient

wind speed. While this functional dependence of the enthalpy transfer coefficient on wind is not supported by observations at low wind speed (Large and Pond 1982), recent experiments with a laboratory apparatus show that this coefficient does indeed increase with wind speed once the latter exceeds about 15 m s^{-1} (Alamaro et al. 2002).

To forecast real events, this atmospheric model is modified in several ways. First, the potential intensity is allowed to vary in time during the integration to reflect variations in potential intensity along the past and forecast track of the storm. (The potential intensity is held fixed across the spatial domain of the model, however.) Second, the sea surface temperature is allowed to vary with time and radius to reflect coupling to the one-dimensional ocean model described in section 2b. Finally, a landfall algorithm is added in which the coefficient of surface enthalpy flux is assumed to vary linearly from unity to zero as the elevation of the coastal plain increases from 0 to 40 m. This procedure is discussed in section 5f.

One advantage of this model is its computational speed: a typical storm can be simulated in less than a minute on a typical desktop computer. It arguably contains all the essential axisymmetric physics necessary for tropical cyclone simulation, only neglecting any departures of the temperature profile from moist adiabatic on angular momentum surfaces and representing the vertical structure of relative humidity by only two layers in the troposphere. Aside from these approximations, the main limitation of the model is its axisymmetry which, among other problems, precludes any direct influence from environmental wind shear, which is known to be a major factor inhibiting tropical cyclone intensification; indeed, statistical analyses show that wind shear is one of the primary predictors of storm intensity change (DeMaria and Kaplan 1994). Based on experience with the coupled model, we have developed a parameterization of shear effects; this is described in section 5c.

b. Ocean model

The axisymmetric hurricane model is coupled to the one-dimensional ocean model developed by Schade (1997). In this model, the mixed layer depth is calculated based on the assumed constancy of a bulk Richardson number, while the mixed layer momentum is driven by surface stress and entrainment. Horizontal advection and the Coriolis acceleration are omitted.

The upper-ocean horizontal velocity and temperature are assumed to have the vertical structure illustrated in Fig. 1 with finite jumps of velocity and buoyancy across the base of the mixed layer. Ignoring horizontal advection and Coriolis accelerations, the time rate of change of the vertically averaged horizontal momentum of the upper ocean is given by

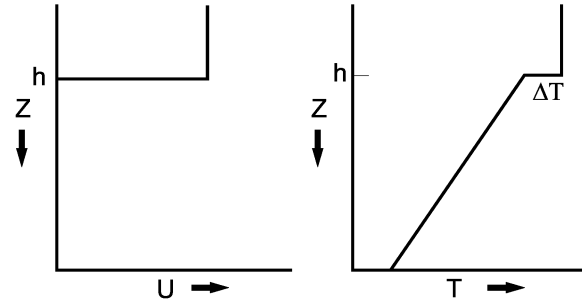


FIG. 1. Assumed (left) kinematic and (right) thermal structure of the upper ocean. The horizontal velocity u and temperature T are assumed to be homogeneous in a mixed layer of thickness h . There is a prescribed jump in temperature, ΔT , across the base of the mixed layer below which the velocity is assumed to vanish and temperature is assumed to decrease linearly with depth.

$$\frac{\partial \rho h u}{\partial t} = |\tau_s|, \quad (2)$$

where ρ is the density of seawater, h is the mixed layer depth (see Fig. 1), u is the magnitude of the mixed layer velocity, and τ_s is the vector wind stress, obtained from the atmospheric model. While (2) describes the changes in mixed layer momentum experienced by an ocean column fixed in space, the atmospheric model requires ocean temperature at its nodes in potential radius coordinates. For ocean columns ahead of the storm, the transformation of (2) into the atmospheric model's potential radius space gives

$$\frac{\partial \rho h u}{\partial \tau} = |\tau_s| + \left(u_r + \frac{\partial r}{\partial \tau} \right) \frac{\partial R}{\partial r} \frac{\partial \rho h u}{\partial R}, \quad (3)$$

where u_r is the translation speed of the storm, the notation $\partial/\partial \tau$ denotes a partial derivative in time at fixed potential radius, and the quantities $\partial r/\partial \tau$ and $\partial R/\partial r$ are deduced from the atmospheric model.

We assume that vertical mixing is the only important effect on temperature during the passage of a tropical cyclone and ignore horizontal advection and surface heat exchange. Price (1981) demonstrates that surface temperature change is usually dominated by mixing, with cooling by surface fluxes a secondary factor. Under these conditions, the vertically integrated enthalpy remains constant:

$$\int_{-\infty}^0 \rho C_i T dz = \int_{-\infty}^0 \rho C_i T_i dz, \quad (4)$$

where C_i is the heat capacity of seawater, T is its temperature, and T_i is the initial temperature. In evaluating the integrals in (4), we approximate C_i and ρ as constants and, as illustrated in Fig. 1, we assume that the temperature lapse rate below the mixed layer is constant. The initial state of the ocean is described using only four quantities: surface temperature, mixed layer depth, the temperature jump ΔT_i at the base of the mixed layer,

and the temperature lapse rate Γ below the mixed layer. The initial mixed layer velocity u is assumed to be zero.

Entrainment into the mixed layer is modeled by assuming that the bulk Richardson number of the mixed layer remains constant (Price 1981). This Richardson number is defined

$$\mathcal{R} \equiv \frac{g\Delta\sigma h}{\sigma u^2},$$

where g is the acceleration of gravity, σ is the potential density, and $\Delta\sigma$ is its jump across the base of the mixed layer. We here ignore pressure and salinity effects on potential density and approximate the bulk Richardson number as

$$\mathcal{R} \approx \frac{g\alpha\Delta Th}{u^2} = \mathcal{R}_{\text{crit}} = 1.0, \quad (5)$$

where α is the coefficient of thermal expansion of seawater, which we approximate by a constant representative of the tropical upper ocean. In this model, we require \mathcal{R} to be equal to a critical value, which we here take to be 1.

Thus, our simplified ocean model consists of (3)–(5). The momentum equation (3) is integrated forward in time, with the surface stress supplied by the atmospheric model. The mixed layer depth h and temperature jump ΔT are then diagnosed using (4) and (5) together with the assumed vertical structure illustrated in Fig. 1.

c. Atmosphere–ocean coupling

In coupling the atmosphere and ocean models it is assumed that a hurricane responds principally to sea surface temperature changes under its eyewall and that these can be closely approximated by sea surface temperature changes under that part of the eyewall that lies along the storm track. Thus, as illustrated in Fig. 2, the ocean response is modeled by a set of one-dimensional ocean columns along the storm track. The sea surface temperature value used by the axisymmetric model is a simple average of the values ahead of and behind the storm at the radius in question. Also, to save computational time, only the columns ahead of and at the center of the storm are calculated and the storm-center sea surface temperature anomaly is used to represent conditions throughout the eye and under the eyewall. While this approximation misses the wake of the storm, where inertial oscillations have a strong influence on mixing (Price 1981), the model cyclone responds most strongly to sea surface temperature anomalies directly under its eyewall and is hardly influenced by temperature anomalies outside its core.

We tested this coupling formulation by comparing simulations based on it with those using the same atmospheric model coupled to the three-dimensional ocean model of Cooper and Thompson (1989), as described in Schade and Emanuel (1999). In those sim-

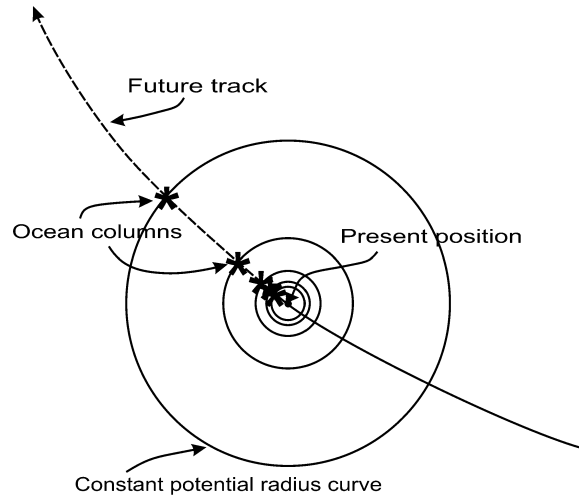


FIG. 2. Configuration of the ocean model. One-dimensional columns are strung out along the future path of the storm at the loci of the intersections of the atmospheric model's potential radius surfaces with the storm track. In a coordinate system moving with the storm center, properties are advected from one ocean column to the next radially inward along the storm track.

ulations, the ocean model was integrated on a regular grid, and the sea surface temperature was interpolated into the potential radius coordinate of the atmospheric model and averaged in azimuth about the storm center. The Cooper–Thompson model is discretized into four layers, but uses the same entrainment closure as the column model used here.

In this test, the tropical cyclone is assumed to be translating in a straight line at a constant speed of 7 m s^{-1} over an ocean with an unperturbed mixed layer depth of 30 m. Figure 3 compares the maximum surface wind speed evolution of three simulations: an uncoupled simulation in which the sea surface temperature is held fixed, a “full physics” simulation in which the complete ocean model is integrated and the surface temperature used by the atmospheric model is averaged in azimuth around the storm center, and a run using the simplified model described above in which the ocean model is integrated only along the path taken by the center of the storm and the sea surface temperatures ahead of and under the eye are used by the atmospheric model. The simplified model does surprisingly well, producing results that are indistinguishable from the simulation using the full ocean model. At translation velocities less than about 4 m s^{-1} , however, the simplified model overestimates the ocean feedback effect and thereby underestimates the maximum wind speed by about 10%.

This comparison demonstrates that vertical turbulent mixing so dominates the physics of sea surface temperature change that all other processes may be neglected during the time between the onset of strong winds and the passage of the eye. While strong vertical mixing is also induced by inertial oscillations excited by the storm, they primarily affect sea surface temper-

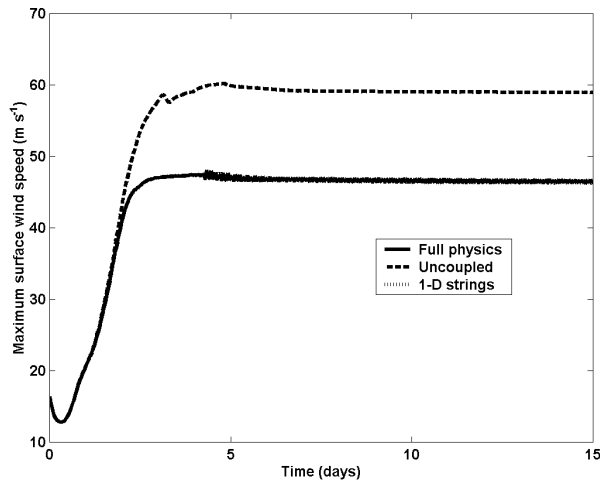


FIG. 3. Evolution with time of the maximum surface wind speed in three different integrations of the coupled atmosphere–ocean model. In each case, the storm is translating uniformly at 7 m s^{-1} over a horizontally homogeneous ocean with an unperturbed mixed layer depth of 30 m. The solid curve shows the results of a simulation coupling the atmospheric model to a three-dimensional ocean model; the dashed line shows the results of a reference run with fixed sea surface temperature, and the dotted curve shows the results of integrating a string of one-dimensional columns along the storm track. In this case, the full physics simulation and the simulation using the string model are very nearly indistinguishable.

atures well to the rear of the storm center, and these have little effect on storm intensity. Indeed, to a good approximation, our atmospheric model is sensitive to surface conditions only under the storm’s eyewall.

We have performed several experiments comparing the full physics and simplified formulations for a variety of initial conditions and translation speeds. These show that the simplified model usually performs quite well. The largest differences between simulations using the full and simplified physics occur for very slow translation speeds ($< 3 \text{ m s}^{-1}$), when neglected processes, such as Ekman pumping, are comparatively important.

3. Data and initialization

In the simulations of real events described presently, the coupled model is supplied with an observed and/or forecast storm track and with information about the prestorm potential intensity, ocean mixed layer depth, submixed layer ocean thermal stratification, and bathymetry/topography along the storm track. In some of the cases presented below, we also supply an estimate of the environmental wind shear along the storm track, used in the formulation described in section 5c. The model is initialized using a synthetic warm-core vortex. In each of the cases discussed below, the geometry of the vortex and the value of the Coriolis parameter are fixed at prescribed values, though in principle they can be varied according to the size and latitude of the real system. The maximum wind speed of this initial vortex is specified to be the “best-track” estimated wind speed

at the beginning of the storm’s life.¹ Given the balance condition of the model, this also effectively initializes the mass (temperature) distribution. On the other hand, the water vapor distribution is not initialized by this procedure, and observations of moisture are generally insufficient for this purpose. But the initial intensification of the storm proves quite sensitive to the initial water vapor distribution, and we make use of this sensitivity to initialize the water vapor (actually, the middle level entropy) based on observations of the rate of change of storm intensity. To accomplish this, the evolution of the model storm’s intensity is at each time step adjusted toward that of the estimated intensity over a fixed interval of time by varying the rate at which low entropy air is injected into the storm’s core in the middle troposphere. That is, to the model’s middle-layer moist entropy equation (see Emanuel 1995a) is added an extra term:

$$\frac{\partial \chi_m}{\partial \tau} = \dots + \gamma(V_{\text{obs}} - V_{\text{sim}})(\chi_m - \chi_{m0}), \quad (6)$$

where χ_m is the middle-level moist entropy variable, χ_{m0} its unperturbed ambient value, the ellipses represent the other terms in the entropy equation, γ is a constant numerical coefficient, V_{obs} is the best-track maximum wind speed, and V_{sim} is the maximum wind speed in the simulation (with a fraction of the translation speed added back; see footnote 1). The effect of this added term is to adjust the entropy of the middle levels of the storm upward or downward in proportion to the difference between the simulated and observed intensity; this in turn drives the storm intensity toward the observational estimate. This procedure insures that the simulated storm is dynamically and thermodynamically self-consistent by demanding consistency with both the observed maximum wind speed and the observed rate of intensity change. The adjustment is implemented during a prescribed interval (usually 1–2 days) for hindcast events and during the whole period up to the current time for real-time forecasts. After the period of adjustment (hereafter, the “matching interval”), the model intensity evolves freely.

For real-time intensity forecasts, the past and predicted storm positions and intensities are taken from official forecasts provided by the National Oceanic and Atmospheric Administration (NOAA) National Hurricane Center (NHC) for Atlantic and eastern Pacific storms and by the U.S. Navy’s Joint Typhoon Warning Center (JTWC) for all other events. When run in “hind-

¹ To account for the contribution of the storm’s translation speed to the maximum wind speed, we subtract a specified fraction of the former from the latter, to obtain the purely circular component of the maximum wind speed. Experience has shown that subtracting the full translation speed from the reported maximum wind speed often results in a system that is too weak. Here we take the specified fraction to be 0.4. In subsequent comparisons of model and observed wind speed, this contribution from the translation speed is added back to the model output.

cast" mode, the model uses best-track data supplied by the two aforementioned centers, except where otherwise stated. Positions and intensities recorded or predicted every 6 hours are linearly interpolated in time to the model's time step. It should be borne in mind that not all of the reported wind speeds are directly measured by aircraft or radar; some are partially subjective estimates based on satellite imagery.

The potential intensity in the Tropics is observed to vary only slowly in time, being governed mostly by sea surface temperature. Therefore, for real-time forecasts, the model's potential intensity is taken from data recorded at the beginning of the storm's life.²

To calculate potential intensity, we use sea surface temperature and atmospheric temperature analyses on a 1° latitude–longitude grid supplied from the National Centers for Environmental Prediction (NCEP), recorded at 0000 UTC near the beginning of the storm's life. The sea surface temperatures used in these analyses are updated weekly, but we do not update them during the life of the storm because storm-induced SST anomalies occasionally affect the analyzed SSTs. Including these in the potential intensity used by the model would result in double counting of the SST feedback since the model produces its own storm-induced anomalies. The potential intensity is calculated from an algorithm described in Bister and Emanuel (2002) and is supplied daily by the Center for Land–Atmosphere Prediction (COLA; maps of potential intensity, generated by COLA, are available online at <http://grads.iges.org/pix/hurpot.html>). For hindcast events, however, we use monthly mean climatological potential intensities. These were calculated using NCEP–National Center for Atmospheric Research (NCAR) monthly mean reanalysis data (Kalnay et al. 1996) from the years 1982–95, inclusive, as described in Bister and Emanuel (2002). The same potential intensity algorithm was used as for the real-time potential intensities. The effects of using monthly mean potential intensity instead of actual potential intensity are explored in section 5e.

The initial state of the ocean along the storm track is described by only two parameters: the ocean mixed layer depth and the temperature gradient just beneath the mixed layer. (We take the initial temperature jump at the base of the mixed layer, ΔT_1 , to have the prescribed value of 0.5 K.) Lacking real-time ocean analyses, we are forced to rely on monthly mean climatology and for this use 1° gridded data from Levitus (1982). (In section 5d we attempt to use sea surface altimetric measurements to modify this mixed layer depth climatology.) Both quantities are linearly interpolated in space to the best track or forecast storm position and in time to the

actual date, assigning the monthly mean climatology to the 15th day of each month.

Bathymetry and topography are specified to ¼° resolution and linearly interpolated to the storm positions. This is used to detect landfall and, also, to reveal places where the ocean mixed layer extends to the sea floor so that surface cooling by mixing cannot occur. As described in section 2a, the landfall algorithm is one of maximum simplicity: The coefficient of surface enthalpy flux decreases linearly with land elevation at the storm center, vanishing over terrain higher than 40 m.

Unless otherwise stated, estimates of the vertical shear of the environmental wind, used in our parameterization of shear effects (section 5c), are those used as real-time input to the Statistical Hurricane Intensity Prediction Scheme (SHIPS), described in DeMaria and Kaplan (1994). These estimates are made by smoothing the spatial distribution of analyzed and forecasted values of the 850–200-hPa horizontal winds so as to remove as much as possible of the shear associated directly with the storm circulation. We make no assertion that the 850–200-hPa wind shear is the optimal quantity to use; it is merely expedient to use these values until and unless superior measures are developed.

In each of the cases presented below, the evolution of maximum surface wind speed in the model is compared to the observed evolution; no attempt has been made to compare the evolutions of model and observed storm structure or precipitation rates.

4. Model performance

The model, named the Coupled Hurricane Intensity Prediction System (CHIPS) for brevity, has been run experimentally at both NHC and JTWC since 2000. Beginning in the 2001 Atlantic season and in September 2002 in the North Pacific, a parameterization of shear effects (described in section 5c) has been included in the forecast model. This parameterization has been successively refined over the last two seasons. Forecast skill has so far been evaluated for Atlantic storms only. The root-mean-square intensity errors of the CHIPS forecasts are comparable to the best statistical forecasts (SHIPS) and smaller than the best deterministic model guidance (Geophysical Fluid Dynamics Laboratory, GFDL). Figure 4 shows results for the 2002 Atlantic hurricane season as an example.

5. Sensitivity to environment and initialization

In this section we illustrate the sensitivity of the coupled model to initial conditions and to various environmental factors. We focus on a limited number of cases, beginning with a single case of a storm that developed and decayed over the central tropical North Atlantic, in which there was virtually no shear and little evidence of significant prestorm upper-ocean thermal anomalies.

² An important motive for not updating the potential intensity is the desire to avoid using analyzed potential intensity that may reflect the presence of the storm in question. The analyzed storm's warm core reduces the analyzed potential intensity that, on the other hand, is supposed to reflect undisturbed environmental conditions.

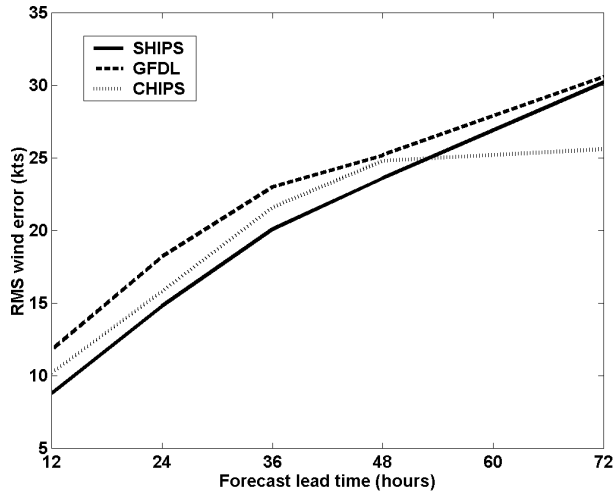


FIG. 4. Root-mean-square intensity errors (kt) for the 2002 Atlantic hurricane season for SHIPS (solid), GFDL hurricane model (dashed), and CHIPS (dotted) forecasts as a function of forecast lead time.

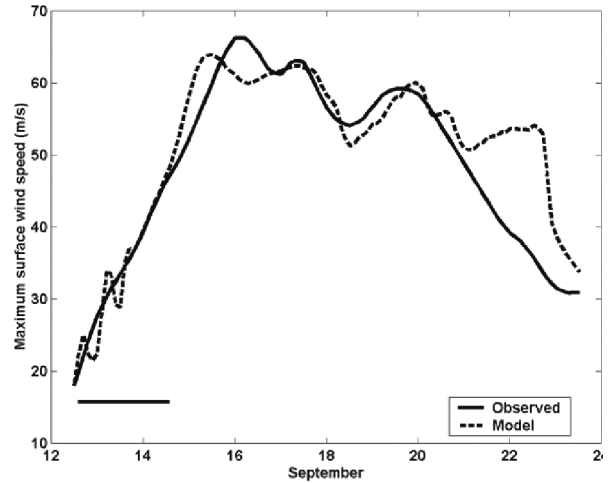
a. The importance of ocean interaction

Hurricane Gert is a good example of model storm behavior when environmental shear is small. Gert developed west of the Cape Verde Islands in mid September 1999 and, after moving west-northwestward for 5 days, turned northward over the central North Atlantic. Figure 5a shows the evolution of the best-track intensity together with a model hindcast. (Real-time forecasts of this system were skillful.) There is good agreement between the observed and predicted intensity. The control forecast is compared in Fig. 5b to another simulation in which ocean feedback is omitted. Forecast errors owing to omission of ocean feedback reach values as large as 25 m s^{-1} on 18 September.

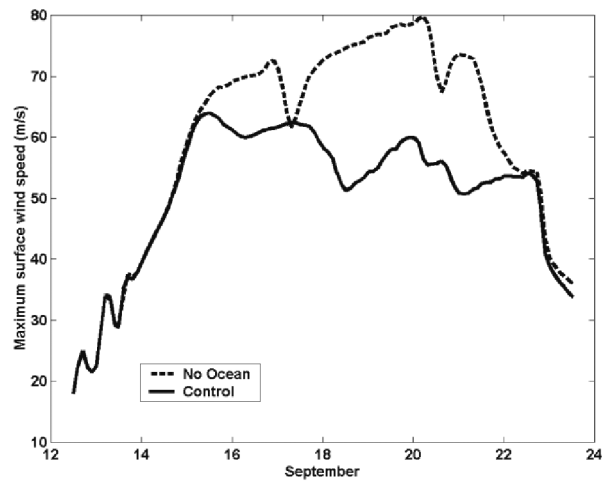
Gert is typical of storms that are relatively unaffected by environmental shear. The ocean mixed layer over which Gert moved was of modest thickness and there was little evidence of significant departures of the pres-torm upper ocean from its monthly climatology. It is our general experience that storms that are not limited by shear, landfall, or declining potential intensity are usually limited to a significant degree by ocean interaction.

b. Sensitivity to initialization

Figure 6a shows the control forecast of Hurricane Gert together with three additional simulations in which, respectively, the matching interval is reduced from 2 days to 12 h, and 3 m s^{-1} is added to and subtracted from all velocities during the matching period. The effects of increasing and decreasing the initial vortex radial size by 30% are illustrated in Fig. 6b. Although there is some sensitivity to these variations, it is not large in this case. We show in section 5c that sensitivity



a



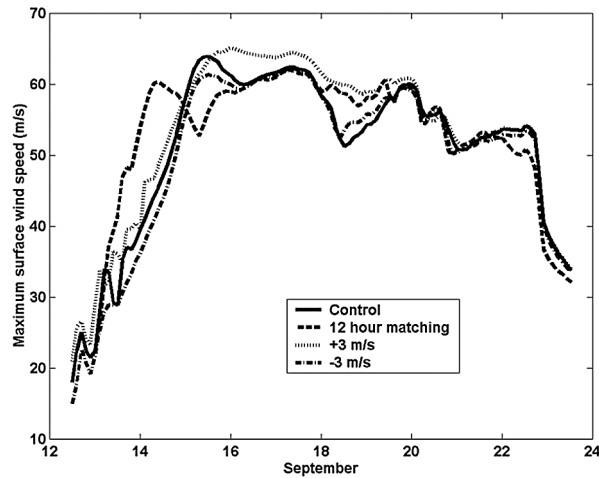
b

FIG. 5. Evolution of maximum wind speed in Hurricane Gert, 1999. (a) Best track (solid) is compared to CHIPS hindcast (dashed). Solid black bar at bottom left shows initialization interval in which the model is matched to observations. (b) As in (a) but without ocean coupling.

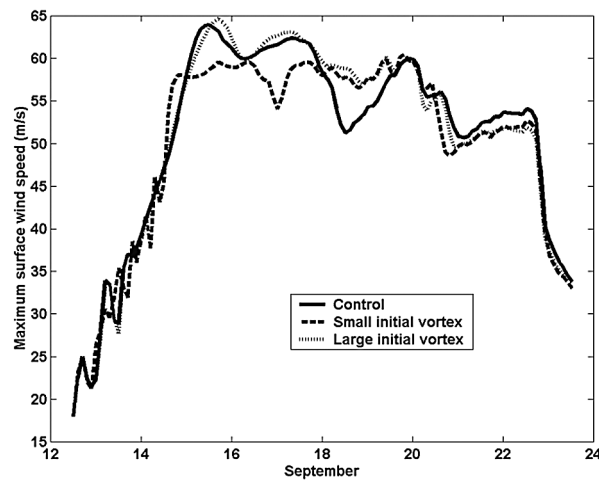
to initialization can be much larger when environmental shear is influential.

c. Vertical shear effects

Although some storms, like Gert, are almost unaffected by environmental shear, the majority of storms suffer to some degree from shear effects. A good example is Tropical Storm Chantal of 2001, which formed just east of the Leeward Islands in mid August and then moved across the central Caribbean, dissipating in the Yucatan on 21 and 22 August. Although Chantal moved through regions of large potential intensity and over deep ocean mixed layers, its maximum winds never ex-



a



b

FIG. 6. Comparison of control forecast (solid) to simulations of Hurricane Gert, 1999, in which (a) the matching interval is decreased to 12 h and the velocities increased and decreased by 3 m s^{-1} during the matching interval and (b) the radial size of the initial vortex is increased and decreased by 30%.

ceeded 60 kt. Figure 7 shows the history of 850–200-hPa environmental shear at the location of Chantal's center.

Figure 8 shows a hindcast of Chantal with the standard configuration of the coupled model. The initialization procedure matches the model to the best track data for 1.5 days, after which the simulation runs freely. For another 36 h, the simulation is quite good, but then departs radically from the best track intensity, attaining an error of about 80 kt by 21 August.

Based on experience simulating sheared storms like Chantal, we developed a parameterization of shear effects. To do this, we first ran a number of simulations in which we matched the storm intensity to the observed

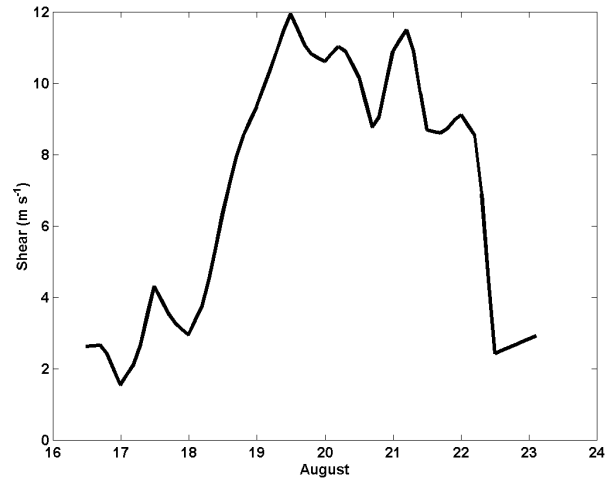


FIG. 7. Evolution of 850–200-hPa shear at the location of the center of Tropical Storm Chantal, 2001.

peak winds for the whole duration of the event, keeping track of the magnitude of the adjustment term on the right side of (6). We then used a multiple regression algorithm to relate this term to model variables and to environmental shear. The resulting parameterization has the effect of ventilating the storm at middle levels, in the nomenclature of Simpson and Riehl (1958), adding a term to the time tendency of middle level entropy of the form

$$\frac{\partial \chi_m}{\partial t} = \dots - \alpha V_{\text{shear}}^2 V_{\text{max}}^2 (\chi_m - \chi_{m0}), \quad (7)$$

where the ellipses represent the other terms in the entropy equation (see Emanuel 1995a), χ_m is the middle-layer moist entropy variable, χ_{m0} is its ambient envi-

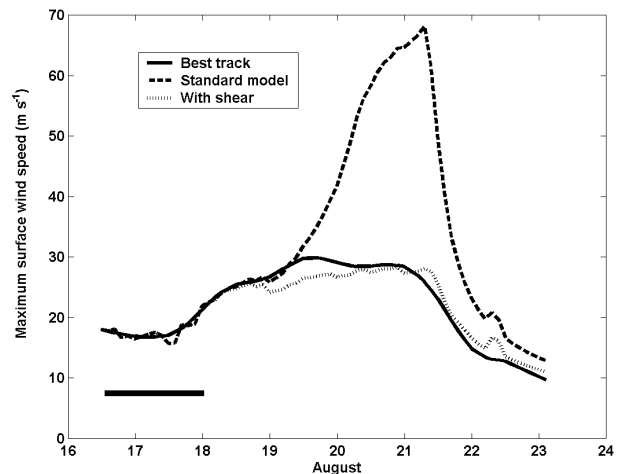


FIG. 8. Evolution of the maximum surface wind speed in Tropical Storm Chantal, 2001. Solid curve shows best-track estimate, dashed curve shows standard model simulation, and dotted curve shows simulation with parameterization of shear included. Solid black bar at bottom left shows initialization interval in which model is matched to observations.

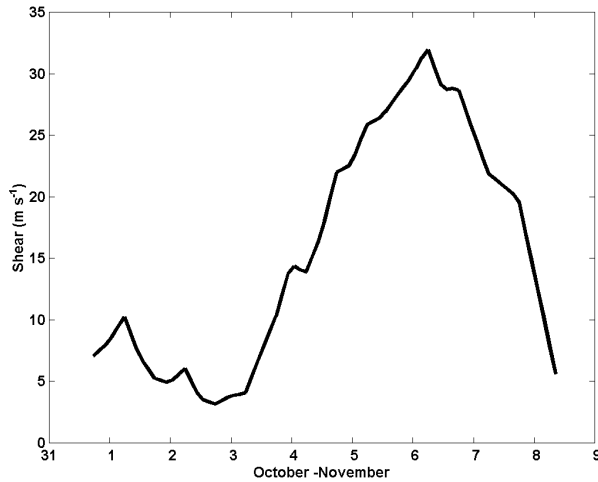


FIG. 9. Evolution of 850–200-hPa shear at the location of the center of Hurricane Michelle, 2001.

ronmental value, α is a numerical coefficient, V_{shear} is the magnitude of the 850–200-hPa shear with the storm itself filtered out, and V_{max} is the maximum surface wind speed. The parameter α and the exponents in (7) were determined by the multiple regression, and the exponents were rounded to the values shown. This should be regarded as an empirical parameterization; we do not here attempt to rationalize its form. In real storms, ventilation is undoubtedly accomplished by asymmetric flows and it is doubtful that the effects of such asymmetries can be represented by a parameterization as simple as (7). Yet, as Fig. 8 shows, a model hindcast with this parameterization switched on is clearly improved over the run without shear.

Another case in which shear played a decisive role is that of Hurricane Michelle in 2001. Michelle was a late season storm, forming over the far western Caribbean around 1 November, then moving northward across western Cuba and northeastward into the central North Atlantic. Figure 9 shows the history of 850–200-hPa shear associated with this event. There was relatively little shear during the first three days, during which Michelle intensified rapidly (Fig. 10). Beginning on 3 November the shear over Michelle's center increased, reaching a peak of over 30 m s^{-1} on 6 November, thereafter declining rapidly. The best-track intensity is compared in Fig. 10 to the simulations with and without the shear parameterization. The standard model, without shear, captures Michelle's intensification quite well, but then continues to intensify the system to about 70 m s^{-1} by 0000 UTC 5 November, whereas the actual storm peaked below 60 m s^{-1} by late on the 3rd. The sudden decline in the simulated intensity starting about 0000 UTC 5 November results from Michelle's passage across western Cuba; after emerging from the north coast of Cuba, the modeled storm reintensifies to about 65 m s^{-1} before finally declining because of decreasing

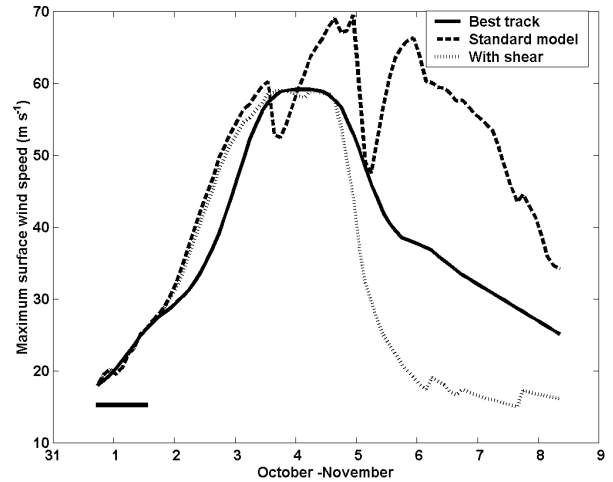


FIG. 10. Evolution of the maximum surface wind speed in Hurricane Michelle, 2001. Solid curve shows best-track estimate, dashed curve shows standard model simulation, and dotted curve shows simulation with parameterization of shear included. Solid black bar at bottom left shows initialization interval in which model is matched to observations.

potential intensity as the storm moved to higher latitudes.

The simulation with the shear parameterization does much better but sends the storm into a somewhat more rapid decline than was observed, perhaps because of the absence of baroclinic interactions in the modeled storm. (According to the National Hurricane Center, Michelle became a vigorous extratropical cyclone around 0000 UTC 6 November.)

While the addition of the shear parameterization clearly improves the model's performance and is critical for producing the good error statistics shown in Fig. 4, it also makes the model somewhat more sensitive, not only to shear magnitude but to initial conditions. Figure 11 demonstrates the large sensitivity of Chantal to shear and initial intensity, with a tendency of the intensities to bifurcate to intense and weak solutions. This appears to be a general characteristic of the model performance when substantial vertical shear is present. We do not know whether this large sensitivity and tendency to bifurcate result from the particular parameterization of shear effects employed here or whether they reflect real sensitivities, but shear clearly reduces the predictability of storm intensity using this model, given the known magnitudes of errors in observed and forecast shear and in observed storm intensity.

Given our assumption that shear affects the storm principally through the ventilation of the core with ambient middle tropospheric air, it is hardly surprising that the evolution of storm intensity in a sheared environment is sensitive to the ambient humidity. Unfortunately, the humidity of the tropical troposphere near the level of minimum entropy is poorly observed; consequently, we use a standard value of relative humidity of 60% to determine the value of χ_{m0} in (7) for all the simulations

reported in this paper. It is apparent from satellite water vapor imagery, however, the moisture is often highly variable in the environments of tropical cyclones. That this can have a strong effect on the intensity of storms in sheared environments is illustrated by Fig. 12, which shows two additional simulations of Tropical Storm Chantal with the middle tropospheric relative humidity reduced to 40% and increased to 80%, respectively. Clearly, lack of knowledge of middle tropospheric humidity will compromise intensity prediction, at least using this model.

d. Upper-ocean variability

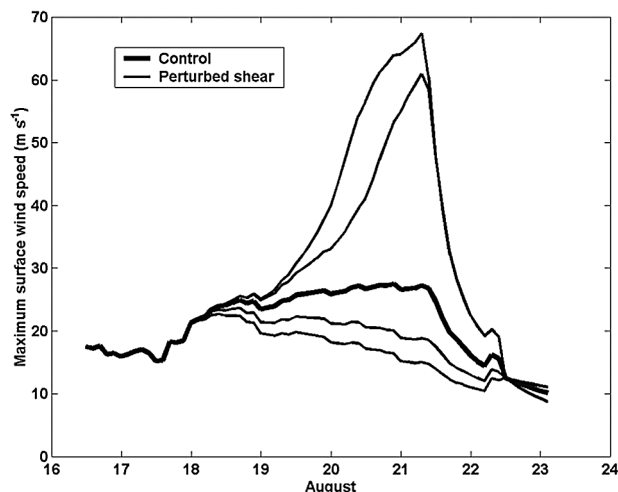
Perturbations from monthly mean climatology of upper-ocean thermal structure can affect the evolution of storm intensity, particularly in places like the Gulf of Mexico where variations in the position of the Loop Current and eddies shed therefrom are common (Schade 1994; Shay et al. 2000). Unfortunately, the paucity of subsurface measurements limits our ability to assess the effect of upper-ocean variability on tropical cyclone intensity evolution. In this section, we describe the effects of modifying monthly mean climatological ocean mixed layer depths using space-based sea surface altimetric measurements.

To modify the climatological mixed layer depths, we use an algorithm developed by Shay et al. (2000), which approximates the upper-ocean density structure as consisting of two constant-density fluid layers with the lower layer taken to be stationary. The assumed absence of horizontal pressure gradients in the lower layer, taken together with hydrostatic equilibrium, dictate that variations in the depth of the interface separating the layers be compensated by variations in sea surface elevation. Interfacial depth anomalies h' are related to sea surface altitude anomalies H' by

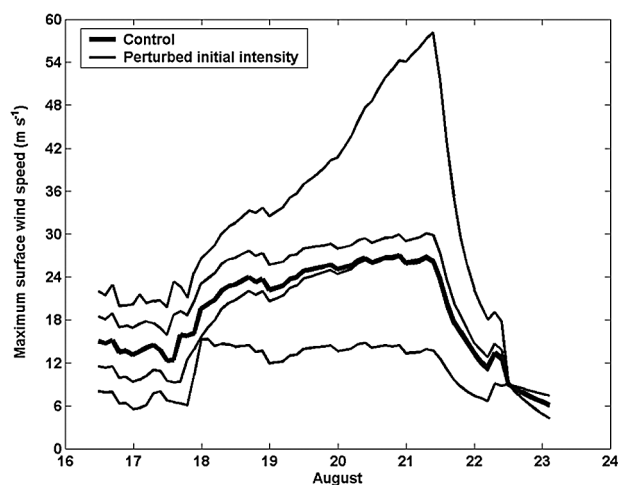
$$h' = \frac{\rho_1}{\rho_2 - \rho_1} H', \quad (8)$$

where ρ_1 and ρ_2 are the densities of the upper and lower layers, respectively.

In reality, several different factors affect departures of sea surface altitude from the geoid. These include tides, barotropic currents, and deep baroclinic structures. Tidal effects can be estimated; otherwise, it is not possible to make unambiguous estimates of upper-ocean density anomalies from altimetry alone. Under circumstances in which density anomalies are concentrated in the uppermost hundred meters or so, however, (8) may be a reasonable approximation. We assume that this is the case in the Gulf of Mexico, where the Loop Current and eddies shed from it have strong effects on upper-ocean density. For the purposes of this analysis, we neglect contributions of salinity to such density anomalies and take the densities in (8) to be specified constants. While this is not likely to be quantitatively ac-



a



b

FIG. 11. Sensitivity of hindcasts of Chantal to magnitude of (a) vertical shear and (b) initial intensity. In both figures, the thick line is the control hindcast. The additional runs perturb the shear by ± 5 and 10 m s^{-1} , and the initial intensity by ± 3 and 6 m s^{-1} during the matching interval of 36 h.

curate, we hope to capture the general effect of upper-ocean thermal anomalies.

To estimate sea surface elevation anomalies, we used data from the Ocean Topography Experiment (TOPEX)-Poseidon mission reduced, corrected, and gridded by The Center for Space Research at the University of Texas at Austin (a detailed description of the data and analysis method is available from the Center for Space Research, at <http://www.csr.utexas.edu/sst/>.) Analyses are available on a 1° latitude-longitude grid and, given the orbital characteristics of the spacecraft, they should be regarded as valid to within about 10 days of the storm

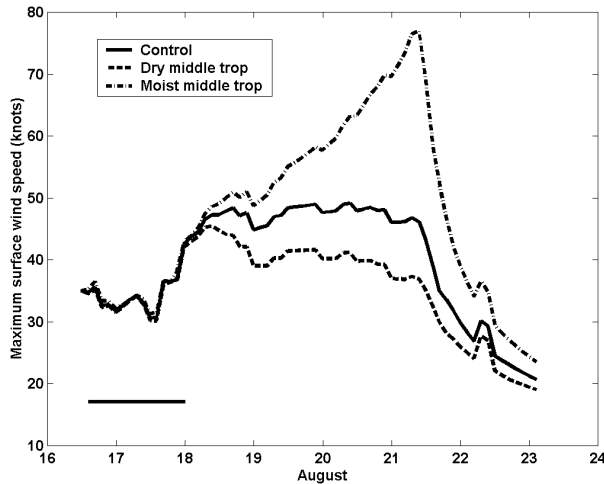


FIG. 12. Sensitivity of hindcasts of Chantal to the assumed environmental relative humidity of the middle troposphere. The solid line shows the control simulation with a relative humidity of 60%, while the dashed and dashed-dotted lines show simulations with the humidity decreased to 40% and increased to 80%, respectively.

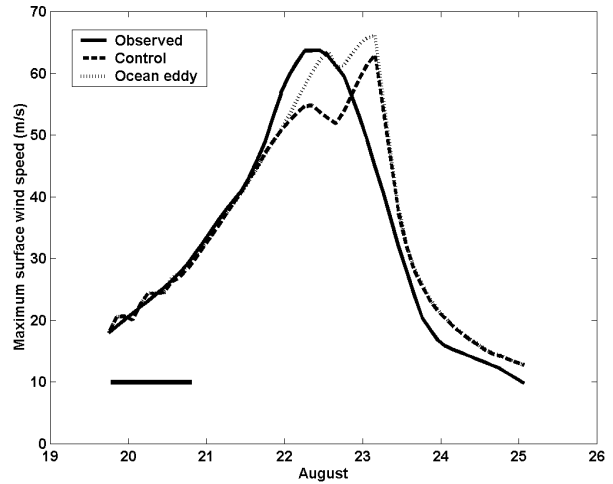


FIG. 13. Modeled and observed intensity evolution of Hurricane Bret, 1999. The dotted curve shows a simulation in which the added heat content of an observed warm eddy has been accounted for using TOPEX–Poseidon altimetry data. Solid black bar at bottom left shows initialization interval in which model is matched to observations.

in question. We linearly interpolate the data in space to the best-track positions of the storms.

The effect of a warm ocean eddy on tropical cyclone intensity is illustrated by the case of Hurricane Bret in 1999. Bret developed in the Bay of Campeche on 19 August and moved northward, parallel to the coast. Mid-day on the 22nd, it began a westward turn that brought it to the southern Texas coast just before midnight. Late on the 21st, it began to be influenced by a warm eddy that had drifted westward across the Gulf after being shed by the Loop Current some months previously.

Figure 13 compares Bret’s best-track intensity evolution to the coupled model hindcast, with and without altimetry-based modifications to the mixed layer depth. (No shear data were available for this event.) Note that the standard model underestimates the peak intensity of the storm but overestimates its intensity at landfall. To produce the third curve in Fig. 13, the monthly climatological ocean mixed layer depth was modified using the altimetry data. The intensity peak is captured better, though at landfall the storm is still more intense than indicated by the best-track record. The added intensity is owing to decreased ocean feedback, which in turn is due to the anomalous upper-ocean heat content of the warm eddy.

In both simulations, the modeled storm undergoes a brief period of rapid intensification just before landfall. As the storm approaches land, the seafloor gradually shoals along the track of the storm, rising to meet the mixed layer base about 18 hours before landfall. After this time, no cold water is present to mix to the surface and the ocean cooling ceases.

Another case in which upper-ocean variability evidently played a role was that of Hurricane Mitch in 1998. Mitch formed in the southern Caribbean in late

October and moved slowly northward and then westward while intensifying rapidly into a category-5 storm. It then turned south and struck Honduras.

The standard coupled model run (without shear) underpredicts Mitch’s peak intensity by more than 15 m s^{-1} (Fig. 14). In addition, there is a secondary intensity peak just before landfall in this and all other simulations, resulting from the shoaling effect discussed above in connection with Hurricane Bret. A positive sea surface height anomaly was clearly present in the TOPEX data; when included using the two-layer formu-

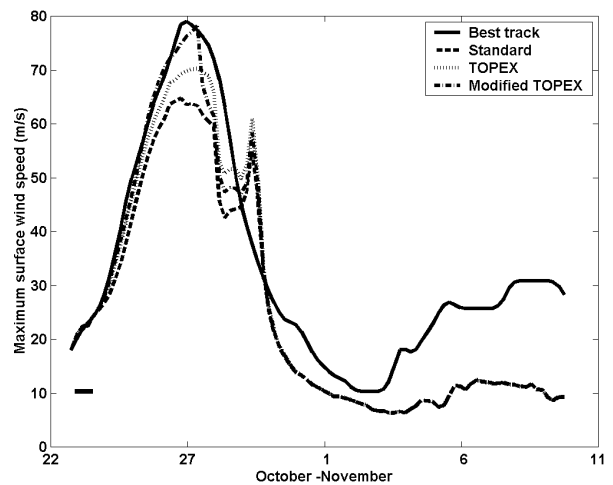


FIG. 14. Modeled and observed intensity evolution of Hurricane Mitch, 1998. The dotted curve shows a simulation in which the added heat content of an observed warm eddy has been accounted for using TOPEX–Poseidon altimetry data. Dashed-dotted curve further modifies the mixed layer depth by attempting to account for the peak eddy amplitude. Solid black bar at bottom left shows initialization interval in which model is matched to observations.

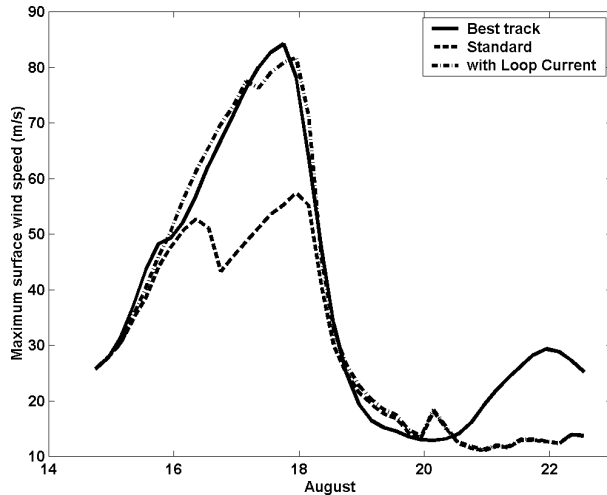


FIG. 15. Modeled and observed intensity evolution of Hurricane Camille, 1969. The dotted curve shows a simulation in which the average upper-ocean structure of the Loop Current had been used throughout. Solid black bar at bottom left shows initialization interval in which model is matched to observations.

lation described above, the simulation is improved, as shown in Fig. 14, though the peak intensity is still underpredicted by more than 10 m s^{-1} .

Examination of the ungridded TOPEX data suggests that Mitch passed directly over the center of a warm ocean eddy. The interpolations used in gridding the data probably reduce the peak height anomaly. We attempted to account for this by increasing the gridded height anomalies at the grid points nearest the eddy center to their observed peak values. The resulting simulation (Fig. 14) is further improved. This suggests that, at least in some cases, upper-ocean measurements with high horizontal resolution may be needed for accurate hurricane intensity prediction.

A particularly dramatic case of historical significance is that of Hurricane Camille of 1969, one of only three Category 5 hurricanes to strike the continental United States since records began. Camille developed in the northwestern Caribbean in mid August, and then moved rapidly northward over the eastern Gulf of Mexico, making landfall at Biloxi, Mississippi, on 17 August. A hindcast with the coupled model (without shear), using monthly climatological upper-ocean conditions (Fig. 15), completely fails to capture Camille's exceptional intensity because of the large ocean cooling that resulted from Camille's passage over the climatologically thin ocean mixed layer of the central Gulf.

One possible factor in this dramatic underprediction is the Loop Current, a warm current that enters the Gulf through the Straits of Yucatan and exits through the Straits of Florida. This current usually flows some distance north into the Gulf before making a hairpin turn eastward and southward. Its width of around 100 km and meandering nature render it poorly represented in the Levitus 1° ocean data. While few direct measure-

ments of the upper Gulf were made around the time of Camille, measurements were made during August in other years. In August 1964, several bathymetric sections were made in the Gulf and are presented in Leipper (1967). We assumed that data from one of these sections (see Leipper's Fig. 12b, p. 190) is representative of Loop Current water and modified the Levitus mixed layer depths and sub-mixed-layer thermal stratification accordingly. We then made the rather extreme assumption that Camille passed right along the axis of the current. This results in a much improved simulation (Fig. 15).

It is clear from these and other simulations we have performed that upper-ocean variability can strongly affect tropical cyclone intensity, even when this variability occurs on scales smaller than 100 km. Accurate forecasting of tropical cyclone intensity, especially in regions like the Gulf of Mexico where small-scale variability is prominent, may require near real-time upper-ocean measurements along the future paths of storms.

e. Effects of variable potential intensity

The hindcast events described above all used potential intensity based on monthly mean NCEP reanalysis data. To explore the effect of departures from this climatology, we ran the coupled model for every tropical cyclone of tropical storm strength or greater in the Atlantic best-track dataset between 1950 and 1997, inclusive, for both the monthly mean and daily potential intensities calculated on a 1° latitude-longitude grid from NCEP reanalysis data. The intent here is to quantify the magnitude of effects owing to potential intensity anomalies, not to assess which approach produces better results. Indeed, since we did not use vertical wind shear in these simulations, many of them contain serious errors. Since shear has a negative effect on storm development, there is a positive bias in the intensities in these simulations, and we believe that this also introduces a positive bias in the magnitude of the difference between simulations with the different potential intensity estimates. Thus we regard the present results as representing an upper bound on the magnitude of the effect.

Figure 16 presents a histogram of root-mean-square intensity errors accumulated over all events, comparing each storm's simulated wind speed to the best-track estimate at the time each storm reached its maximum intensity. There is a slight, but statistically insignificant decrease in rms error when daily values of potential intensity are used. There is no significant decrease in the number of very large errors. We did encounter a small number of events for which the departures of potential intensity from monthly mean climatology were large and had a correspondingly large effect on simulated storm intensity. The most extreme case in our dataset was that of Hurricane Floyd in 1981 for which the difference between the simulated intensities using the daily and monthly mean potential intensities was as

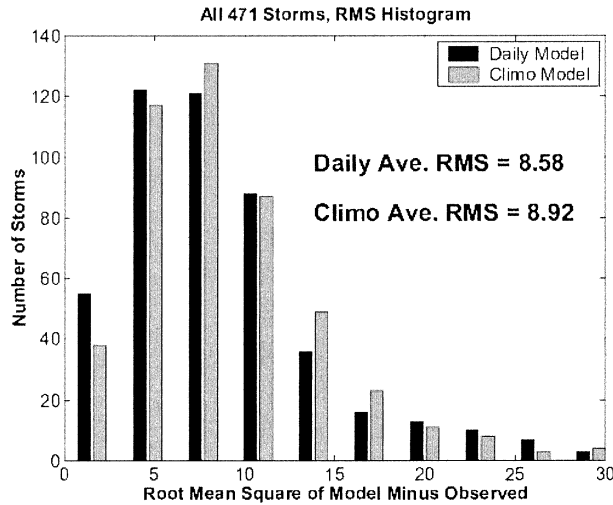


FIG. 16. Histogram showing the number of cases as a function of the magnitude of the rms wind speed error, measured at the time of the peak wind speed during each event, according to the best-track data for all 471 storms. The gray bars show errors using monthly climatological potential intensity, while the black bars show errors using daily values estimated from NCEP reanalysis data.

large as 30 m s^{-1} , while the potential intensities themselves differed by as much as 25 m s^{-1} .

f. Terrain characteristics

A simple landfall algorithm—setting the enthalpy exchange coefficient to zero everywhere at the time the storm center crosses the coast—was found to work quite well in most cases, accurately reproducing the observed rapid decline in intensity. When storms pass over low, swampy terrain, however, the model systematically overpredicts the rate of decline of maximum winds. We attribute this to the transfer of enthalpy from wet ground and shallow water, as discussed briefly by Emanuel (1999) and more extensively by Shen et al. (2002). To further quantify this effect, we have coupled the atmospheric model described here in section 2a to a simple layer of standing water with an initial temperature equal to the unperturbed sea surface temperature experienced by the storm just before landfall and whose subsequent thermal evolution is determined strictly by turbulent surface enthalpy exchange. Radiative effects are ignored. We run this model under idealized conditions in which the storm translation speed is constant, as is the potential intensity; for these idealized simulations we turn off coupling to the ocean.

The intensity evolutions in these idealized simulations are shown in Fig. 17 for landfall over dry land and over standing water of various depths. These simulations, which are broadly consistent with those of Shen et al. (2002), demonstrate that even a few tens of centimeters of water can significantly reduce the rate of decline of storm intensity.

These results suggest that accurate prediction of in-

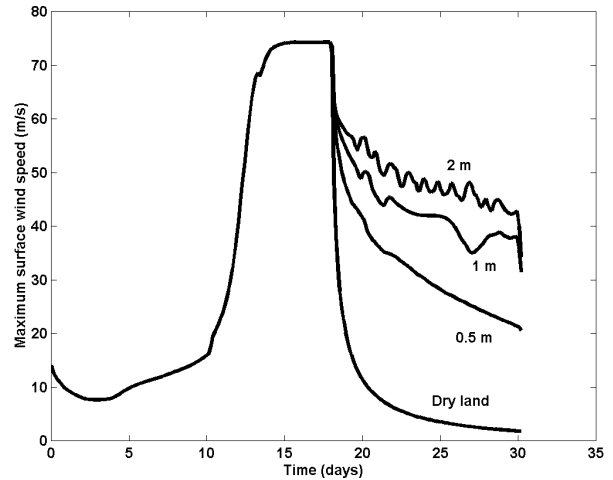


FIG. 17. Evolution of maximum wind speed in idealized, uncoupled simulations in which the translation speed and potential intensity are constant. In each simulation landfall occurs at 18 days. The bottom curve pertains to dry land; the other curves are labeled with the depth of standing water.

tensity evolution after landfall may depend in part on an accurate specification of land surface properties, such as soil moisture and temperature, and the properties of any standing water, such as swamps, marshes and lakes. To avoid having to incorporate large databases containing such characteristics, we devised a crude algorithm that assumes that the amount of standing water is a simple, linear function of topography. Rather than setting the surface enthalpy exchange coefficient to zero when the storm center crosses the coastline, we allow it to decrease linearly with surface altitude, vanishing when the altitude reaches 40 m. We do not advocate this procedure as a substitute for the detailed specification of land surface properties, but include it here to demonstrate that even a crude proxy for surface effects can make a large difference to the evolution of tropical cyclones over land.

A case in point is that of Hurricane Andrew in 1992. Andrew developed in the central tropical North Atlantic in mid August and moved northwestward to a position east of the Bahamas. During the first five days of its life, its intensity was suppressed by environmental wind shear. Beginning on 22 August, Andrew underwent rapid intensification, striking south Florida with winds close to 70 m s^{-1} . It then traversed the southern part of the peninsula, emerging into the Gulf of Mexico about 6 hours after landfall. After crossing the Gulf, Andrew made a second landfall in Louisiana on 25 August.

The portion of south Florida over which Andrew passed is comprised largely of the Everglades, an extensive swamp. Figure 18 compares Andrew's best-track intensity evolution to that of the standard model and an additional simulation in which the enthalpy flux coefficient was set to zero over land. (No shear data were available for this event. To achieve a reasonable sim-

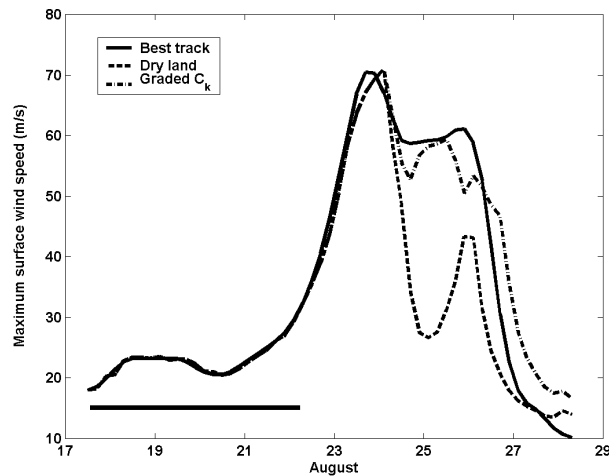


FIG. 18. Evolution of the maximum surface wind speed in Hurricane Andrew, 1992. Solid curve shows best-track estimate, dashed curve shows model simulation in which the enthalpy exchange coefficient is zero over land, and dashed-dotted curve shows simulation with the exchange coefficient decreasing linearly with increasing surface altitude. Solid black bar at bottom left shows initialization period in which the model is matched to observations.

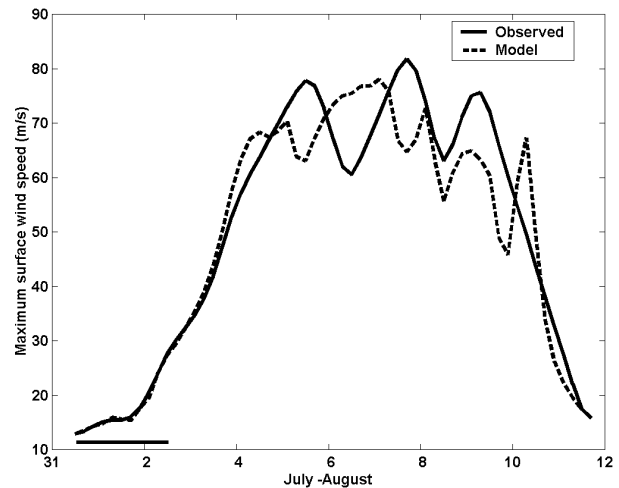


FIG. 19. Evolution of the maximum surface wind speed in Hurricane Allen, 1980. Solid curve shows best-track estimate, dashed curve shows model simulation. Solid black bar at bottom left shows initialization period in which model is matched to observations.

ulation, the matching interval was extended over much of the early life of the storm, during which it was strongly affected by shear.) The two simulations differ greatly after landfall in south Florida. Our crude algorithm clearly improves the intensity hindcast, though it underpredicts the rate of decline of Andrew's intensity after landfall in Louisiana.

Although our land surface flux algorithm is crude, these results, taken together with the more detailed analysis of Shen et al. (2002), clearly demonstrate the importance of accounting for land surface characteristics in predicting tropical cyclone intensity evolution over land.

g. Internal variability

Although we have proceeded under the premise that most observed intensity variations of tropical cyclones arise from interaction with their environment, it is well known that internal features such as concentric eyewall cycles are often associated with large intensity fluctuations. It is not always clear whether eyewall cycles themselves result strictly from internal instabilities or whether they are triggered and/or controlled by environmental interactions. Here we attempt to simulate Hurricane Allen of 1980, which had several eyewall replacement cycles, as documented by Willoughby et al. (1982). The results of this simulation are compared to observations in Fig. 19. As in the observed storm, the simulation of Allen undergoes several intensity oscillations that in some ways resemble concentric eyewall cycles. [The ability of this model to produce concentric eyewall-like phenomena was documented by Emanuel (1995a).] While the amplitude of these oscillations is

similar to that of the observed cycles, their phase seems randomly related to the observed phase. As might be expected, the phase of the predicted oscillations proves quite sensitive to environmental and initial conditions, suggesting that the modeled phenomenon is indeed an internal instability. Detailed examination of the model fields reveals little in the way of environmental perturbations along Allen's track: the potential intensity was nearly constant and, although Allen passed close to land masses (e.g., Jamaica), the model has no way of simulating land interactions unless the storm center passes over land. This further supports the idea that the intensity fluctuations in the simulation of Allen are indeed internally driven.

6. Summary

A simple coupled model has been used to explore the sensitivity of tropical cyclone intensity evolution to initialization and to a variety of environmental factors. Although the atmospheric component of the model is axisymmetric and therefore cannot directly include environmental wind shear, we developed and tested a parameterization of shear that attempts to account for the ventilation of low entropy air through the storm core at mid levels. The coupled model with the shear parameterization was run experimentally at the National Hurricane Center and at the Joint Typhoon Warning Center and, in the Atlantic region, was found to be about as skillful as statistical forecasts and better than other deterministic guidance. Experience with the model shows it to perform well when there is little environmental shear and when storms move over an ocean whose upper thermal structure does not depart much from climatology. Under these conditions, the model is not overly sensitive to the way in which it is initialized, but in most

circumstances the coupling to the ocean is crucial to obtain good results. When substantial shear is present, on the other hand, the modeled intensity proves sensitive both to the magnitude of the shear itself and to initial and environmental conditions and shows a tendency toward bimodal intensity distributions. This supports the experience of hurricane forecasters, who place great emphasis on the importance of shear. These results suggest that forecasts are rendered increasingly uncertain in the presence of shear, unless the shear is so strong as to prevent development in any reasonable environment. A potentially important source of uncertainty when substantial shear is present is the poorly observed humidity of the middle troposphere.

Accurate forecasts of tropical cyclone intensity require not only good forecasts of environmental winds but good knowledge of upper-ocean thermal structure. Although we could only show a few cases here, we have encountered quite a few events in which climatological upper-ocean thermal conditions were inadequate for accurate intensity prediction. We believe that the importance of tropical cyclone intensity prediction justifies the inclusion of upper-ocean temperature and salinity measurements in routine airborne reconnaissance missions.

Bathymetry is important where water depths are sufficiently small to limit the downward increase of mixed layer depths by entrainment, as may happen where sea-floors shoal gradually toward coastlines or where storms approach the coast obliquely.

With the exception of a very small percentage of storms, we have not found much systematic difference between forecasts made using real-time potential intensity and those made using monthly climatological potential intensity. This perhaps reflects the relatively small interannual variability of sea surface temperatures in tropical cyclone-prone regions.

The spindown of storms after landfall appears to be affected by the presence of standing water, such as swamps and lakes, and is probably similarly affected by soil moisture content and, perhaps, soil temperature. Detailed forecasts of tropical cyclone evolution over land probably require accurate specification of land surface characteristics.

In a few cases, notably that of Hurricane Allen in 1980, we found evidence of important internal variability, mostly taking the form of concentric eyewall cycles. Because such cycles have comparatively short time scales, they are not predictable responses to environmental fluctuations and, as such, they compromise the overall predictability of storm intensity. In our limited experience, this mode of variability appears mostly in intense storms that remain in benign environments for long periods; otherwise, storm intensity is mostly controlled by its environment. It should be noted that not all eyewall replacement cycles that occur in this model develop spontaneously; some occur in response

to strong environmental stimulation, such as passage over an island or peninsula.

The axisymmetry of our atmospheric model precludes the simulation of baroclinic effects such as trough interactions, which are often cited as primary causes of intensity change (e.g., Molinari and Vollaro, 1989, 1990, 1995). The undersimulation of Hurricane Michelle's late stage intensity (Fig. 10) suggests that such interactions can indeed be important. Our coupled model may prove an ideal tool for isolating such effects, as it attempts to account for most of the other processes thought to be important; thus baroclinic effects may be a major source of systematic error. This will be the subject of future work by our group.

Finally, we caution against considering the various environmental influences on storm intensity as operating independently from each other. For example, shear, in suppressing storm intensity, also suppresses ocean feedback; the sudden cessation of shearing can then lead to more rapid intensification and, briefly, to greater intensity than could have been reached had shear been absent altogether. These, and similar effects, are also the subject of continuing investigation by our group.

Acknowledgments. The authors thank Dr. Lars Schade for providing his coupled model and advice on using it; Hugh Willoughby for helpful advice and comments; Ed Rappaport, Fiona Horsfal, and Michelle Mainelli for their help in running CHIPS at the National Hurricane Center; Buck Sampson of the Monterey Naval Research Laboratory; and Don Schiber, Donald Laframboise, Chris Cantrell, and Steve Vilpors of the Naval Pacific Meteorology and Oceanography Center for assistance in running CHIPS at the Joint Typhoon Warning Center. We are also grateful for helpful comments from two anonymous reviewers.

REFERENCES

- Alamaro, M., K. Emanuel, J. Colton, W. McGillis, and J. B. Edson, 2002: Experimental investigation of air-sea transfer of momentum and enthalpy at high wind speed. Preprints, *25th Conf. on Hurricanes and Tropical Meteorology*, San Diego, CA, Amer. Meteor. Soc., 667-668.
- Bender, M. A., and I. Ginis, 2000: Real-case simulations of hurricane-ocean interaction using a high-resolution coupled model: Effects on hurricane intensity. *Mon. Wea. Rev.*, **128**, 917-946.
- Bister, M., and K. A. Emanuel, 1998: Dissipative heating and hurricane intensity. *Meteor. Atmos. Phys.*, **50**, 233-240.
- , and —, 2002: Low frequency variability of tropical cyclone potential intensity 2. Climatology for 1982-1995. *J. Geophys. Res.*, **107**, 4621, doi:10.1029/2001JD000780.
- Cooper, C., and J. D. Thompson, 1989: Hurricane-generated currents on the outer continental shelf. Part I: Model formulation and verification. *J. Geophys. Res.*, **94**, 12 513-12 539.
- DeMaria, M., and J. Kaplan, 1994: A statistical hurricane intensity prediction scheme (SHIPS) for the Atlantic basin. *Wea. Forecasting*, **9**, 209-220.
- , and —, 1997: An operational evaluation of a statistical hurricane intensity prediction scheme (SHIPS). Preprints, *22d Conf. on Hurricanes and Tropical Meteorology*, Fort Collins, CO, Amer. Meteor. Soc., 280-281.

- Emanuel, K. A., 1986: An air–sea interaction theory for tropical cyclones. Part I: Steady-state maintenance. *J. Atmos. Sci.*, **3**, 585–605.
- , 1988: The maximum intensity of hurricanes. *J. Atmos. Sci.*, **45**, 1143–1155.
- , 1995a: The behavior of a simple hurricane model using a convective scheme based on subcloud-layer entropy equilibrium. *J. Atmos. Sci.*, **52**, 3959–3968.
- , 1995b: Sensitivity of tropical cyclones to surface exchange coefficients and a revised steady-state model incorporating eye dynamics. *J. Atmos. Sci.*, **52**, 3969–3976.
- , 1999: Thermodynamic control of hurricane intensity. *Nature*, **401**, 665–669.
- Frank, W. M., and E. A. Ritchie, 2001: Effects of vertical wind shear on the intensity and structure of numerically simulated hurricanes. *Mon. Wea. Rev.*, **129**, 2249–2269.
- Gallacher, P. C., R. Rotunno, and K. A. Emanuel, 1989: Tropical cyclogenesis in a coupled ocean–atmosphere model. Preprints, *18th Conf. on Hurricanes and Tropical Meteorology*, San Diego, CA, Amer. Meteor. Soc., 121–122.
- Jones, S. C., 2000: The evolution of vortices in vertical shear. Part III: Baroclinic vortices. *Quart. J. Roy. Meteor. Soc.*, **126**, 3161–3185.
- Kalnay, E., and Coauthors, 1996: The NCEP/NCAR 40-Year Reanalysis Project. *Bull. Amer. Meteor. Soc.*, **77**, 437–471.
- Khain, A., and I. Ginis, 1991: The mutual response of a moving tropical cyclone and the ocean. *Beitr. Phys. Atmos.*, **64**, 125–141.
- Large, W. G., and S. Pond, 1982: Sensible and latent heat flux measurements over the ocean. *J. Phys. Oceanogr.*, **12**, 464–482.
- Leipper, D. F., 1967: Observed ocean conditions and Hurricane Hilda, 1964. *J. Atmos. Sci.*, **24**, 182–196.
- Levitus, S., 1982: *Climatological Atlas of the World Ocean*. NOAA Prof. Paper 13, 173 pp. and 17 microfiche.
- Molinari, J., and D. Volaro, 1989: External influences on hurricane intensity. Part I: Outflow layer eddy angular momentum fluxes. *J. Atmos. Sci.*, **46**, 1093–1105.
- , and —, 1990: External influences on hurricane intensity. Part II: Vertical structure and response of the hurricane vortex. *J. Atmos. Sci.*, **47**, 1902–1918.
- , and —, 1995: External influences on hurricane intensity. Part III: Potential vorticity structure. *J. Atmos. Sci.*, **52**, 3593–3606.
- Nong, S., and K. Emanuel, 2003: Concentric eyewalls in hurricanes. *Quart. J. Roy. Meteor. Soc.*, **129**, 3328–3338.
- Price, J. F., 1981: Upper ocean response to a hurricane. *J. Phys. Oceanogr.*, **11**, 153–175.
- Raymond, D. J., 1995: Regulation of moist convection over the west Pacific warm pool. *J. Atmos. Sci.*, **52**, 3945–3959.
- Schade, L. R., 1994: The ocean’s effect on hurricane intensity. Ph.D. thesis, Massachusetts Institute of Technology, 127 pp.
- , 1997: A physical interpretation of SST-feedback. Preprints, *22d Conf. on Hurricanes and Tropical Meteorology*, Fort Collins, CO, Amer. Meteor. Soc., 439–440.
- , and K. A. Emanuel, 1999: The ocean’s effect on the intensity of tropical cyclones: Results from a simple coupled atmosphere–ocean model. *J. Atmos. Sci.*, **56**, 642–651.
- Schubert, W. H., and J. J. Hack, 1983: Transformed Eliassen-balanced vortex model. *J. Atmos. Sci.*, **40**, 1571–1583.
- Shay, L. K., G. J. Goni, and P. G. Black, 2000: Effects of a warm oceanic feature on Hurricane Opal. *Mon. Wea. Rev.*, **128**, 1366–1383.
- Shen, W., I. Ginis, and R. E. Tuleya, 2002: A numerical investigation of land surface water on landfalling hurricanes. *J. Atmos. Sci.*, **59**, 789–802.
- Shutts, G. J., 1981: Hurricane structure and the zero potential vorticity approximation. *Mon. Wea. Rev.*, **109**, 324–329.
- Simpson, R. H., and H. Riehl, 1958: Mid-tropospheric ventilation as a constraint on hurricane development and maintenance. *Proc. Tech. Conf. on Hurricanes*, Miami Beach, FL, Amer. Meteor. Soc., D4-1–D4-10.
- Willoughby, H. E., and P. G. Black, 1996: Hurricane Andrew in Florida: Dynamics of a disaster. *Bull. Amer. Meteor. Soc.*, **77**, 643–652.
- , J. A. Clos, and M. G. Shoreibah, 1982: Concentric eyes, secondary wind maxima, and the evolution of the hurricane vortex. *J. Atmos. Sci.*, **39**, 395–411.